

Zero-age main-sequence radii and luminosities as analytic functions of mass and metallicity

Christopher A. Tout,[★] Onno R. Pols, Peter P. Eggleton and Zhanwen Han[†]

Institute of Astronomy, The Observatories, Madingley Road, Cambridge CB3 0HA

Accepted 1996 February 6. Received 1996 February 2; in original form 1995 October 30

ABSTRACT

We present fitting formulae for the zero-age main-sequence radii and luminosities of stars as functions of their masses and metallicities. The formulae cover masses from 0.1 to 100 M_{\odot} and metallicities from $Z=0.0001$ to 0.03. Within this range the functions are everywhere strictly analytic. They take the form of rational functions in mass with only positive coefficients calculated as polynomials in metallicity. Errors are generally less than 7.5 per cent for luminosity and less than 5 per cent for radius. For a solar metallicity of $Z=0.02$ these errors are less than 3 per cent for luminosity and 1.2 per cent for radius.

Key words: stars: fundamental parameters – Hertzsprung–Russell (HR) diagram.

1 INTRODUCTION

Since Eggleton, Fitchett & Tout (1989) published a set of formulae describing the evolution of radius and luminosity of Population I stars as a function of mass and age there has been some demand for similar formulae for Population II stars. In this paper we present the first and most important step towards such formulae. In addition to including metallicity as an independent variable, the new formulae represent two other substantial improvements over the old set. First, the full stellar models have been computed using the most modern physics as reported by Pols et al. (1995). Secondly, the formulae are strictly analytic everywhere within the valid range. In particular, this means that they are continuous and differentiable in both mass and metallicity. This differentiability is particularly important where number counts of stars, such as luminosity functions, are being analysed. For instance, the relation between luminosity function and mass function depends directly on the gradient of the mass–luminosity relation (see, e.g., Kroupa, Tout & Gilmore 1990).

2 STELLAR MODELS

We have calculated a grid of zero-age main-sequence stellar models using the most recent version of the evolution pro-

gram of Eggleton (1971, 1972, 1973) described by Pols et al. (1995). In order to avoid discontinuous derivatives caused by the linear interpolation in opacities at low temperatures, we have used bicubic spline interpolation (routines E01DAF and E02DEF from Numerical Algorithms Limited, Oxford, NAG) for these models. We constructed models for each of the metallicities for which we have opacity tables from Rogers & Iglesias (1992, OPAL) and Alexander & Ferguson (1994), $Z=0.0001, 0.0003, 0.001, 0.004, 0.01, 0.02$ and 0.03. The hydrogen abundance was chosen to make the excess helium abundance over primordial proportional to the metallicity, so that helium abundance $Y=0.24+2Z$ and hydrogen abundance $X=0.76-3Z$. If we take $X_{\odot}=0.7$ and $Z_{\odot}=0.02$, the above metallicities correspond to $[\text{Fe}/\text{H}]=\log_{10}(Z/Z_{\odot})-\log_{10}(X/X_{\odot})=-2.337, -1.859, -1.335, -0.728, -0.319, 0$ and 0.195 respectively. The mixture of metals is that derived from Solar system meteorites by Anders & Grevesse (1989). For each metallicity we calculated 600 models with masses from 0.1 to 100 M_{\odot} , equally spaced in $\log M$. The evolution code explicitly follows the CNO elements. For stars of mass greater than about 1.5 M_{\odot} , CNO burning begins in the central core during pre-main-sequence evolution. We mimic this by a device which we developed mainly by trial and error. Starting with the absolute zero-age mixture at 0.1 M_{\odot} , we ‘evolve’ up the main sequence with time by adding mass. At each time-step the mass of the model is increased to $M'=\sqrt[599]{1000}M$, where M is the current mass, so that the 600th model has mass 100 M_{\odot} . The time-step is chosen to be $\Delta t=5\tau_{\text{KH}}(M/M_{\odot})$, where τ_{KH} is the Kelvin–Helmholtz time-scale. The heat term $-TDS/Dt$ (where T is the temperature and S the entropy)

[★]Present address: Space Telescope Science Institute, 3700 San Martin Drive, Baltimore, MD 21218, USA.

[†]Present address: Centre for Astrophysics, University of Science and Technology of China, Hefei, Anhui, 230026, China.

is not included in the energy equation, so that the models are always in thermal equilibrium. The reactions of the CNO cycle are allowed to proceed at their appropriate rates to determine the new carbon and oxygen abundances, but the consumption of hydrogen and production of helium by either the pp chain or the CNO cycle is not permitted. The nitrogen abundance is then adjusted so that X , Y and Z are maintained at their zero-age values. The procedure is hindered by the fact that very massive stars ($20 M_{\odot}$ or more) have burnt proportionately less oxygen when they reach the main sequence than intermediate-mass stars (about $2 M_{\odot}$). However, the main sequences that we obtain always pass within 1 per cent in luminosity and radius of the zero-age points of pre-main-sequence tracks for stars evolved from well before any CNO or hydrogen burning has begun. The differences are largest for the high metallicities and become insignificant at the lowest metallicities.

3 METHOD OF FITTING

The primary aim was to produce simple and computationally efficient but accurate empirical fits, that are continuous and differentiable, to theoretical stellar models over the range of stellar masses and metallicities encountered observationally. To this end we followed Eggleton et al. (1989) and attempted to fit luminosity L and radius R as a function of mass M for $Z=0.02$ using rational polynomials. Unfortunately, the desire for only integer powers had to be relaxed and, in order to obtain satisfactory fits, we had to introduce the square root of the mass in eight places. We were able to fit the luminosity to better than 3 per cent over the whole range by

$$L = \frac{\alpha M^{5.5} + \beta M^{11}}{\gamma + M^3 + \delta M^5 + \epsilon M^7 + \zeta M^8 + \eta M^{9.5}}, \quad (1)$$

where the coefficients α , β etc. are given in the first column of Table 1. For the radius

$$R = \frac{\theta M^{2.5} + \iota M^{6.5} + \kappa M^{11} + \lambda M^{19} + \mu M^{19.5}}{\nu + \xi M^2 + \omicron M^{8.5} + M^{18.5} + \pi M^{19.5}}, \quad (2)$$

with the coefficients given in the first column of Table 2, fits within 1.2 per cent over the whole range. In each case we found the power indices by eye and trial and error, while the coefficients were found by minimizing the squares of the differences in $\log L$ or $\log R$ between the formula and each of the 600 models using the NAG routine E04FDF.

The next step was to use the same formulae for other metallicities but allow the coefficients to vary, hopefully as little as possible given that similar structure exists in the relations whatever the metallicity. Note that it is important that the coefficients remain positive to ensure that the rational functions remain analytic for all positive M and Z . The procedure was immediately successful for the luminosity formula, but some of the coefficients in the radius fit varied enormously, by two or three orders of magnitude, because different terms in the functions began to model different parts of the relation at different metallicities. As expected, such variation proved unacceptable for the next stage of the fitting procedure. To avoid it and successfully stabilize the procedure, the coefficient ν was fixed at its optimum value at $Z=0.02$ for all metallicities.

The final step was to fit the coefficients α to π , excluding ν , as functions of metallicity. We employed simple polynomials in $\log_{10}(Z/Z_{\odot})$ that best preserved the accuracy of

Table 1. Coefficients for equation (3).

	a	b	c	d	e
α	0.39704170	-0.32913574	0.34776688	0.37470851	0.09011915
β	8.52762600	-24.41225973	56.43597107	37.06152575	5.45624060
γ	0.00025546	-0.00123461	-0.00023246	0.00045519	0.00016176
δ	5.43288900	-8.62157806	13.44202049	14.51584135	3.39793084
ϵ	5.56357900	-10.32345224	19.44322980	18.97361347	4.16903097
ζ	0.78866060	-2.90870942	6.54713531	4.05606657	0.53287322
η	0.00586685	-0.01704237	0.03872348	0.02570041	0.00383376

Table 2. Coefficients for equation (4).

	a'	b'	c'	d'	e'
θ	1.71535900	0.62246212	-0.92557761	-1.16996966	-0.30631491
ι	6.59778800	-0.42450044	-12.13339427	-10.73509484	-2.51487077
κ	10.08855000	-7.11727086	-31.67119479	-24.24848322	-5.33608972
λ	1.01249500	0.32699690	-0.00923418	-0.03876858	-0.00412750
μ	0.07490166	0.02410413	0.07233664	0.03040467	0.00197741
ν	0.01077422	0	0	0	0
ξ	3.08223400	0.94472050	-2.15200882	-2.49219496	-0.63848738
\omicron	17.84778000	-7.45345690	-48.96066856	-40.05386135	-9.09331816
π	0.00022582	-0.00186899	0.00388783	0.00142402	-0.00007671

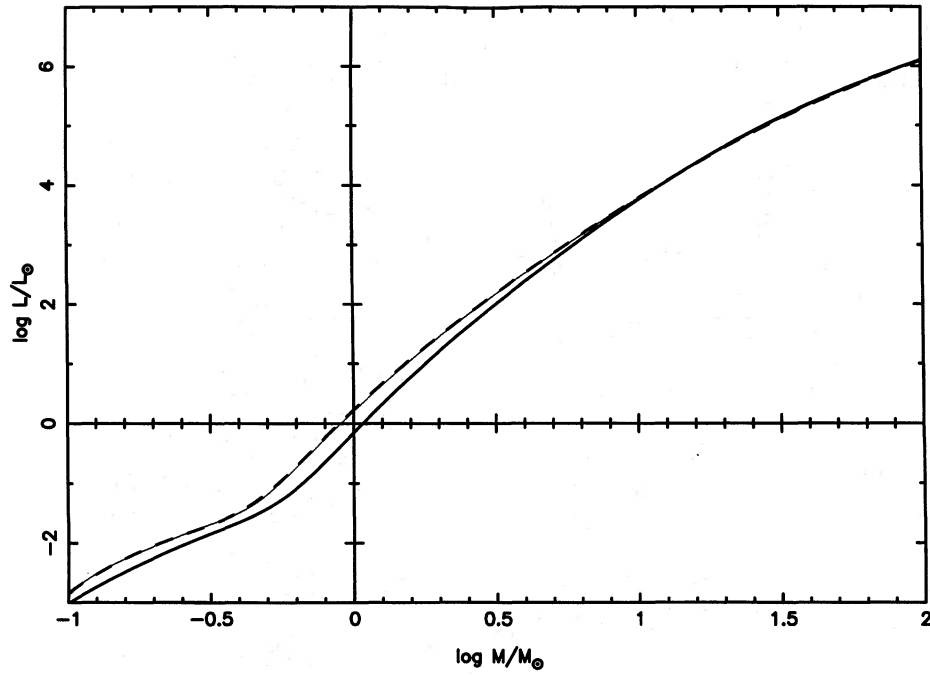


Figure 1. The mass–luminosity relations, equation (1), for $Z=0.02$ (solid line) and $Z=0.0003$ (broken line). Dots are the positions of the 600 detailed structure models. In the case of $Z=0.02$ they all are hidden by the line.

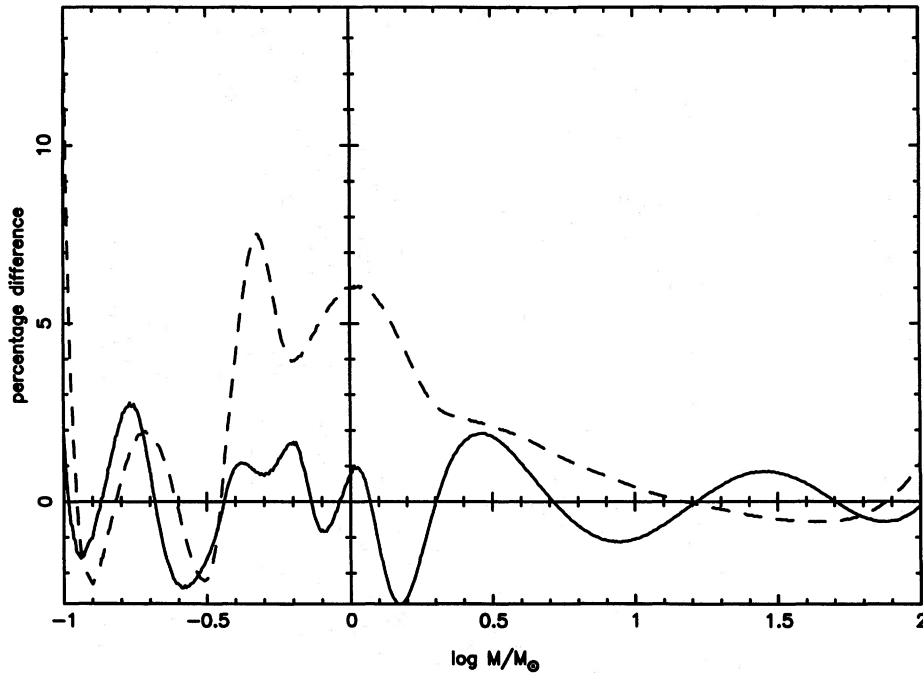


Figure 2. The percentage errors between the luminosity fits, equation (1), and the detailed models for $Z=0.02$ (solid line) and $Z=0.0003$ (broken line).

the independent fits without overfitting in Z . This required quartics for both luminosity and radius, but in each case we forced the polynomials to pass through the best-fitting values for $Z=0.02$. Thus the formulae for luminosity coefficients are of the form

$$\alpha = a + b \log_{10}(Z/Z_{\odot}) + c [\log_{10}(Z/Z_{\odot})]^2 + d [\log_{10}(Z/Z_{\odot})]^3 + e [\log_{10}(Z/Z_{\odot})]^4, \quad (3)$$

and for the radius coefficients

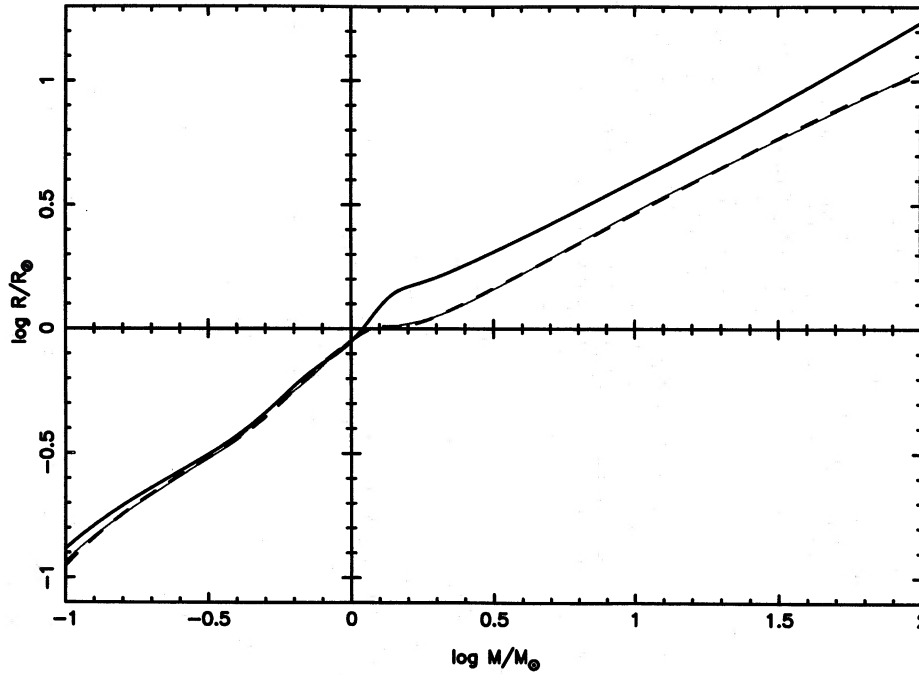


Figure 3. The mass–radius relations, equation (2), for $Z=0.02$ (solid line) and $Z=0.001$ (broken line). Dots are the positions of the 600 detailed structure models.

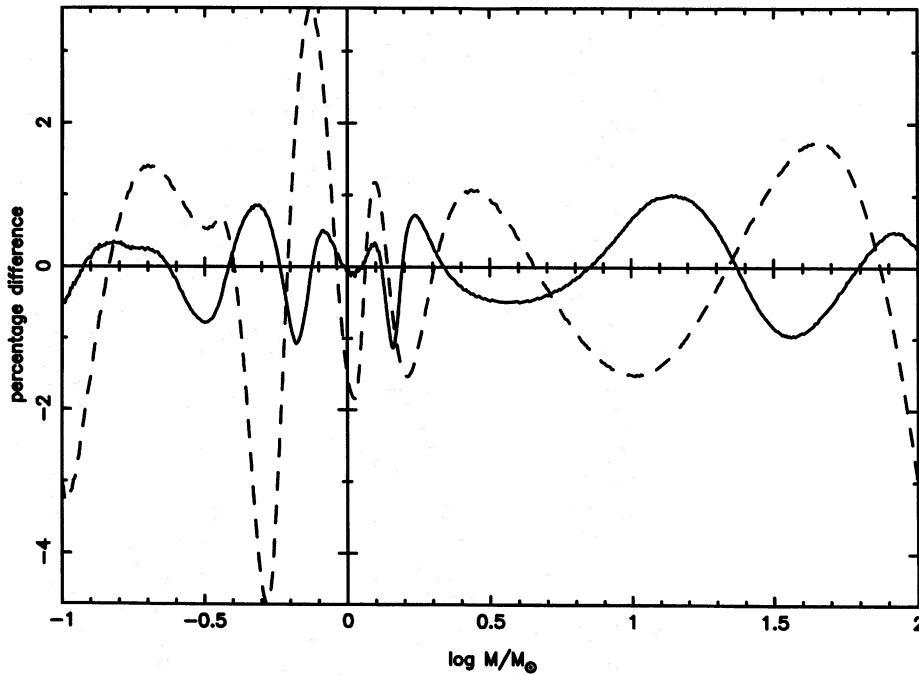


Figure 4 The percentage errors between the radius fits, equation (2), and the detailed models for $Z=0.02$ (solid line) and $Z=0.001$ (broken line).

$$\theta = a' + b' \log_{10}(Z/Z_{\odot}) + c' [\log_{10}(Z/Z_{\odot})]^2 + d' [\log_{10}(Z/Z_{\odot})]^3 + e' [\log_{10}(Z/Z_{\odot})]^4. \quad (4)$$

Note that in each case the constants a and a' give the coefficients for solar metallicity, $Z=0.02$. For each coefficient $\alpha \dots$ the best-fitting coefficients $a \dots$ were obtained by a further least-squares minimization using the NAG routine

E02ADF. The coefficients for luminosity and radius are listed in Tables 1 and 2 respectively.

4 RESULTS

We consider the formulae to be satisfactory if they are able to reproduce the detailed-model luminosities and radii

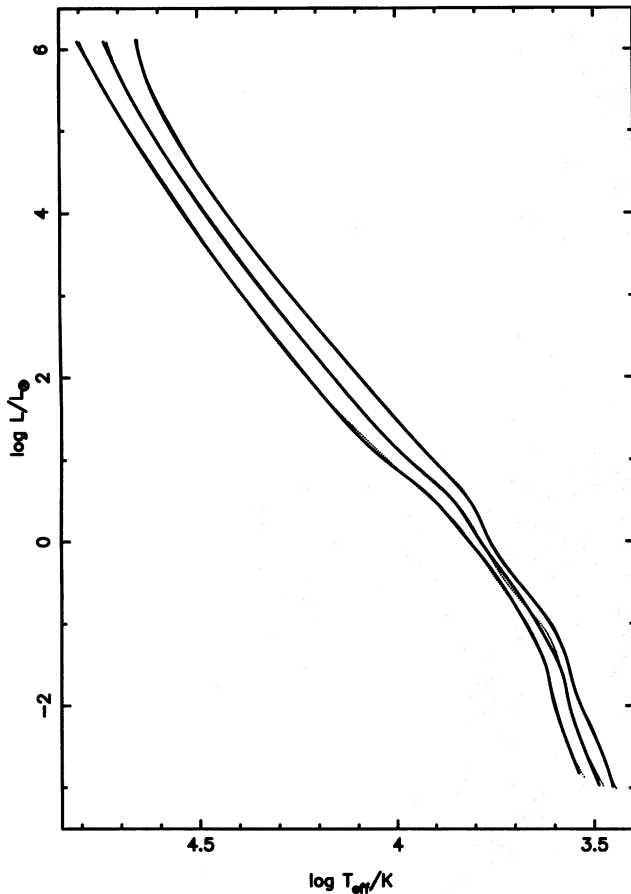


Figure 5. The Hertzprung–Russell diagram zero-age main-sequence tracks for $Z=0.03$ (uppermost), 0.004 and 0.0001 (lowest). Solid lines are obtained from equations (1) and (2), while dots are the detailed models.

within 10 per cent over the whole range of masses and metallicities, with the expectation that the errors will be much smaller for metallicities near solar. The worst errors occur at the low-mass end ($0.1 M_{\odot}$) in luminosity and between 0.5 and $2 M_{\odot}$ in radius, and generally for the lowest metallicities. Fig. 1 illustrates the best- and the worst-fitting curves for luminosity, while Fig. 2 gives the percentage error in these fits. In fact, the worst error of all is about 14 per cent at $M=0.1 M_{\odot}$ for $Z=0.0003$, but for $M > 0.1035$ the error is always less than 7.5 per cent. Figs 3 and 4 are the same, but for radius. In this case the worst error of almost 5 per cent occurs at $M=0.52 M_{\odot}$ for $Z=0.001$. Fig. 5 shows the positions of three zero-age main sequences in the Hertzsprung–Russell diagram. We have also investigated the errors in the first derivatives with respect to mass by differentiating the formulae (1) and (2) analytically to give $d \log L/d \log M$ and $d \log R/d \log M$. The expressions obtained can be compared with approximations to the derivatives found by differencing consecutive models. All the major features are reproduced, and in general the differences do not exceed 10 per cent in the case of luminosity. The generally smaller gradients in radius and the very sharp change in gradient at about $1.33 M_{\odot}$ (modelled as a discontinuity by Eggleton et al. 1989) mean that differences between estimated and fitted $d \log R/d \log M$ are larger. Fig. 6 illustrates this for $Z=0.02$. Fortunately, this gradient is less important than $d \log L/d \log M$.

5 CONCLUSIONS

We have produced and described a set of easily computable analytic formulae for the zero-age main-sequence luminosity and radius of stars as functions of metallicity in the range $Z=0.0001$ to 0.03 and mass in the range $M=0.1$ to $100 M_{\odot}$. The formulae are continuous and differentiable

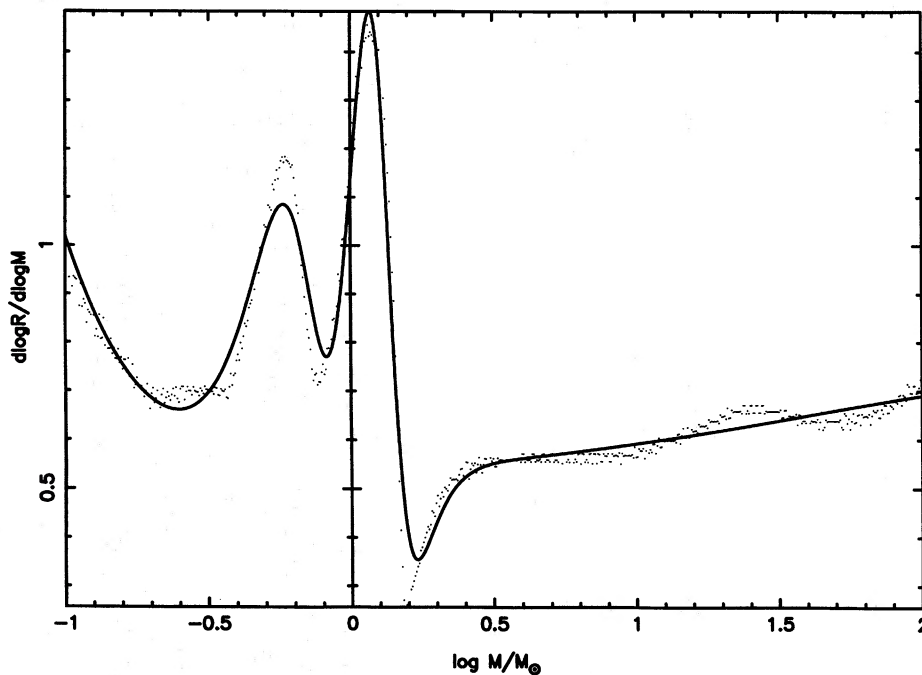


Figure 6. The gradient of the mass–radius relation, equation (2), with respect to mass for $Z=0.02$ (solid line). Dots are approximations to the actual derivatives found by differencing consecutive models.

within this range. Although they should not be extrapolated outside the fitted range, extrapolation in mass will give only inaccurate but still reasonable numbers. On the other hand, extrapolation in metallicity should be avoided at all costs, because the nature of the fitting allows the coefficients in the rational functions to become negative outside the fitted range, with disastrous consequences for continuity in mass. In order to avoid typing errors when using these formulae, we are very happy to provide upon request electronic copies of routines that evaluate them.

ACKNOWLEDGMENTS

CAT and ORP are very grateful to PPARC for support from fellowships, and ZH thanks the Institute of Astro-

nomy, Cambridge for assistance. Some Starlink resources have been used in the preparation of this manuscript.

REFERENCES

- Alexander D. R., Ferguson J. W., 1994, *ApJ*, 437, 879
Anders E., Grevesse N., 1989, *Geochim. Cosmochim. Acta*, 53, 197
Eggleton P. P., 1971, *MNRAS*, 151, 351
Eggleton P. P., 1972, *MNRAS*, 156, 361
Eggleton P. P., 1973, *MNRAS*, 163, 279
Eggleton P. P., Fitchett M. J., Tout C. A., 1989, *ApJ*, 347, 998
Kroupa P., Tout C. A., Gilmore G., 1990, *MNRAS*, 244, 76
Pols O. R., Tout C. A., Eggleton P. P., Hans Z., 1995, *MNRAS*, 274, 964
Rogers F. J., Iglesias C. A., 1992, *ApJS*, 79, 507